Wrinkled Graphenes: A Study on the Effects of Synthesis Parameters on Exfoliation–Reduction of Graphite Oxide

ARTICLE *in* THE JOURNAL OF PHYSICAL CHEMISTRY C · JULY 2011

Impact Factor: 4.77 · DOI: 10.1021/jp204039k

5 AUTHORS, INCLUDING:

Adarsh Kaniyoor
Trinity College Dublin
23 PUBLICATIONS **504** CITATIONS
SEE PROFILE

Tessy Baby
Indian Institute of Technology Madras
31 PUBLICATIONS **832** CITATIONS
SEE PROFILE

T. Arockiadoss
Indian Institute of Technology Madras
20 PUBLICATIONS **424** CITATIONS
SEE PROFILE

N. Rajalakshmi
88 PUBLICATIONS **1,964** CITATIONS
SEE PROFILE

THE JOURNAL OF PHYSICAL CHEMISTRY C

ARTICLE

pubs.acs.org/JPCC

Wrinkled Graphenes: A Study on the Effects of Synthesis Parameters on Exfoliation-Reduction of Graphite Oxide

Adarsh Kaniyoor,[†] Tessy Theres Baby,[†] Thevasahayam Arockiadoss,[†] Natarajan Rajalakshmi,[‡] and Sundara Ramaprabhu*[,†]

[†]Alternative Energy and Nanotechnology Laboratory (AENL), Nano Functional Materials Technology Centre (NFMTC), Department of Physics, Indian Institute of Technology Madras (IITM), Chennai 600036, India

[‡]Centre for Fuel Cell Technology (ARCI), IIT Madras Research Park, Taramani, Chennai 600 113, India

Supporting Information

ABSTRACT: In the present work, we have systematically investigated the effect of different exfoliation conditions on the synthesis of graphene from graphite oxide (GO). Four different conditions were used to exfoliate GO: Ar @ 1050 °C, vacuum @ 200 °C, H_2 + Ar mixture @ 200 °C, and H_2 @ 200 °C. Few layered graphenes obtained by these methods were characterized by thermogravimetry, diffractometry, spectroscopy, microscopy, surface, and elemental analysis techniques. New insights obtained upon a detailed analysis of these are presented. Although the morphology and characteristics of these graphenes are similar, differences are observed in the amount of functional groups present, resulting in considerable change in their electrical properties. These results show conclusively that the atmosphere for exfoliation of GO plays a critical role in low temperature syntheses of graphene. It is observed that exfoliation-reduction of GO in pure hydrogen atmosphere at 200 °C results in the highest quality of a few layered graphene sheets.

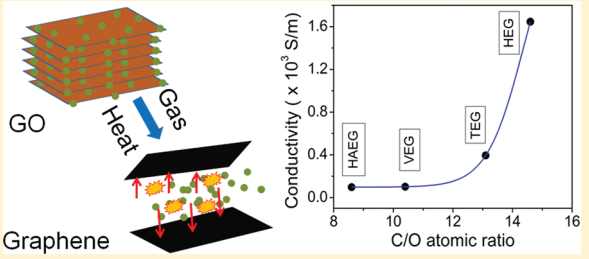

1. INTRODUCTION

Graphene is the 2D one atom thick allotrope of carbon and is the building block of most of the other forms of carbon. It can be wrapped into 0D fullerenes, folded into 1D carbon nanotubes, and stacked to get 3D graphite. Because of its peculiar properties, graphene has received tremendous scientific interest from theoreticians as well as experimentalists. The unusual energy dispersion relation of single-layer graphene wherein the low-lying electrons behave like massless Dirac fermions gives rise to unique phenomena such as quantum spin Hall effect,[1] enhanced Coulomb interaction,[2] suppression of the weak localization,[3] and deviation from the adiabatic Born−Oppenheimer approximation.[4] Its extraordinary high carrier mobility at room temperature,[5,6] conductance quantization,[7] possibilities of inducing a band gap through the lateral quantum confinement,[8] and prospects for epitaxial growth[9] make graphene a promising material for future electronic circuits. In addition, closely packed graphene sheets could be employed in applications such as transparent conductors,[10] field emission displays,[11] and composite materials.

Minute quantities of single layer graphene were first obtained by mechanical cleavage of highly oriented pyrrolitic graphite,[5] a technique developed by Novoselov et al. Since then, many different synthesis techniques have been developed. Most of these techniques are top down approaches, that is, conversion of 3D graphite to 2D graphene. A few of these techniques are micro mechanical cleavage, liquid phase exfoliation of graphite in various solvents by ultrasonication,[12] intercalation of graphite,[13] microwave irradiation,[14] exfoliation of graphite oxide (GO) by "gasothermal",[15−18] solvothermal,[19−22] and photothermal[23,24] methods, etc. The bottom up approaches include growth of graphene from precursor gases via techniques like chemical vapor deposition (CVD),[25−27] microwave plasma enhanced chemical vapor deposition (MPECVD),[28] etc. Mechanical cleavage technique involves repeated peeling of graphite using scotch tape or a similar mechanism. Clearly, this manual process is arduous and hard to control and optimize. However, it is to be noted that the graphene obtained by this method is excellent and hence is useful for studying fundamental science. A few CVD techniques have also been developed for synthesis of single layer graphene. The graphene obtained is not free-standing and has to be transferred to suitable substrates for further studies. Sample contamination due the catalyst layer is also a possibility. Techniques such as liquid phase exfoliation, intercalation-exfoliation, acid treatment, etc., suffer from low yield of monolayer graphene and in most cases result in nanoplatelets having larger (>10) number of layers. In contrast, GO-based exfoliation techniques can be used to obtain large quantities of few layered graphene (∼5 layers) and are therefore useful from an application point of view. Such graphenes have excellent properties like high surface area, good thermal and electrical conductivities, and good catalytic activity.

Received: May 1, 2011
Revised: August 1, 2011
Published: August 08, 2011

In this Article, we investigate the effect of different exfoliation conditions on the properties of the synthesized graphenes. GO was synthesized from two different graphite precursors using two methods, the Hummers method and the modified Hummers method. Four different exfoliation conditions were followed: Ar @ 1050 °C, vacuum @ 200 °C, H_2 + Ar mixture @ 200 °C, and H_2 @ 200 °C. We prefer to call these techniques "gasothermal" methods because they are based on the exfoliation-reduction of GO in various gaseous atmospheres and at different temperatures. The graphenes obtained from GO are highly wrinkled and hence can also be called "wrinkled graphenes". The characteristics of wrinkled graphenes such as diffraction patterns, Raman and IR fingerprints, surface area, elemental composition, etc., will be discussed and compared. Furthermore, we present some simple modifications to the above techniques so as to allow facile and large-scale synthesis of graphene. We believe that this kind of systematic study of exfoliated graphenes would help graphene researchers, worldwide. In addition, this study will also show that wrinkled graphenes consisting of a few layers of graphene can be envisaged as viable alternatives for single layer graphene.

2. EXPERIMENTAL METHODS

2.1. Materials. Expandable graphite, SP-1, 45 μm with 99.99% purity was mostly used for graphene synthesis. Larger size graphite particles were obtained from Alfa Aesar (99.9%, 10 mesh). Sodium nitrate ($NaNO_3$, 99.5%), potassium permanganate ($KMnO_4$, 99.5%), and concentrated sulphuric acid (98%) were purchased from Rankem chemicals, India. Sodium chloride (NaCl, 99.9%) was purchased from SRL, India. Hydrogen peroxide (30%) was procured from S D Fine-Chem Ltd. India. Deionized (DI) water was used for all reactions.

2.2. Synthesis of Exfoliated Graphenes. Exfoliated graphenes were prepared in two stages. The first step involved conversion of graphite to graphite oxide. Two different graphites were used: SP graphite (SPGr) and Alfa Aesar graphite (AAGr). AAGr was ball milled for 12 h to get fine particles. Two methods were adopted for GO synthesis: Hummers method (HGO) and a modified Hummers method (MHGO), the details of which are given in our earlier report.[18] The resultant GOs were labeled as SPHGO, SPMHGO, AAHGO, and AAMHGO. Thereafter, these GOs were exfoliated and reduced to graphene by the following exfoliation techniques. Thermally exfoliated graphene (TEG) was synthesized according to the report of Schniepp et al.[15] A small amount of GO was taken in a quartz boat and introduced into a preheated (1050 °C) tubular furnace. Argon atmosphere was maintained inside the furnace. The sudden increase in temperature (~2000 °C/min) resulted in exfoliation of GO to graphene. Vacuum exfoliation (VEG) was based on the method developed by Wei et al.[16] However, unlike their method, an in-house developed Sieverts apparatus[29] was used for exfoliation. GO was loaded in the sample cell, and high vacuum (10^{-6} mbar) was created. Under vacuum, GO was heated at 200 °C for 5 h. Hydrogen−argon exfoliated graphene (HAEG) was synthesized as follows. A small amount of GO was taken in a quartz boat and introduced into a tubular furnace. The furnace was flushed with Ar for 15 min, and the temperature was raised to 200 °C. At 200 °C, H_2 was allowed in the presence of argon. Exfoliation occurred in less than 1 min, but the flow of gases was continued for 30 min. Hydrogen exfoliated graphene (HEG) was synthesized on the basis of our previous report.[18] The quartz tube with GO placed inside was flushed with Ar for 15 min, followed by H_2 for 5 min at room temperature (30 °C). The temperature was raised to 200 °C in the presence of H_2. At 200 °C, exfoliation occurred immediately, but the flow of H_2 was continued for another 30 min. The furnace was allowed to cool naturally to room temperature. Graphene was also synthesized using AAHGO and AAMHGO.

2.3. Characterizations. Differential scanning calorimetry was carried out on DSC 200 PC, PHOX, NETZSCH under N_2 atmosphere at a heating rate of 5 °C/min. Thermogravimetric (TGA) studies were carried out using a Perkin-Elmer, TGA 6 analyzer. Powder X-ray diffraction studies were carried out using a PANalytical X'PERT Pro X-ray diffractometer with nickel-filtered Cu Kα radiation as the X-ray source in the 2θ range of 5−90° with a step size of 0.016°. UV−Visible absorption spectra of GO and different graphenes were recorded on a JASCO Corp., V-570 spectrophotometer. The solvent used for dissolving the samples was ethanol. Identification and characterization of functional groups were carried out using a Perkin-Elmer FT-IR spectrometer in the range 500−4000 cm^{-1}. The samples were prepared via a KBr pellet method. The Raman spectra were obtained with a WITec alpha 300 Confocal Raman system equipped with a Nd:YAG laser (532 nm) as the excitation source. Field emission scanning electron microscopy and transmission electron microscopy images were obtained using FESEM, FEI QUANTA, and JEOL TEM-2010F instruments. Brunauer−Emmett−Teller (BET) surface area analysis was determined by recording nitrogen adsorption/desorption isotherms at 77 K using a static volumetric technique with a Micromeritics ASAP V3.01 G 2020 instrument. For solution-phase surface area measurements, methylene blue (MB) sock solution was prepared in ethanol. Different amounts of HEG were dispersed by ultrasonication in 10 mL aliquots taken from the stock solution, and their absorbance was noted using spectrometer. X-ray photoelectron spectroscopy (XPS) analysis was performed with a SPECS GmbH spectrometer (Phoibos 100MCD Energy Analyzer) using Al Kα radiation (1486.6 eV). The residual pressure inside the analysis chamber was in the 10^{-10} mbar range. The spectrometer was calibrated by using photoemission lines of Ag (Ag $3d^{3/2}$ = 367 eV with reference to Fermi level). Peaks were recorded with constant pass energy of 20 eV at 100 W power. XPS signals were analyzed using CASA XPS software. The samples for XPS were prepared by dispersing the samples in water and drop casting on Si substrates. Electrical conductivity of the samples at room temperature were measured using the four-probe arrangement connected to a Keithley 2400 source meter and interfaced to a computer using LabView.

3. RESULTS AND DISCUSSION

3.1. Graphite Oxide: Thermal Behavior and Reduction to Graphene. Graphite oxide is a nonstoichiometric compound with the degree of oxidation being specific to the synthesis conditions and procedures. The particle size of the initial graphite used affects the physical appearance of GO obtained. The photograph in Figure 1 shows the four different GOs prepared. The GO obtained from AA graphite (AAHGO and AAMHGO) has a flake-like appearance, whereas GO obtained from SP graphite (SPHGO and SPMHGO) can easily be crushed into powder form. The use of AAGr is time-consuming because it has to be ball milled to get small particles. Graphite with smaller sizes can solve this problem. Hence, most of the studies were carried out on SPGr-based graphenes, unless otherwise mentioned.

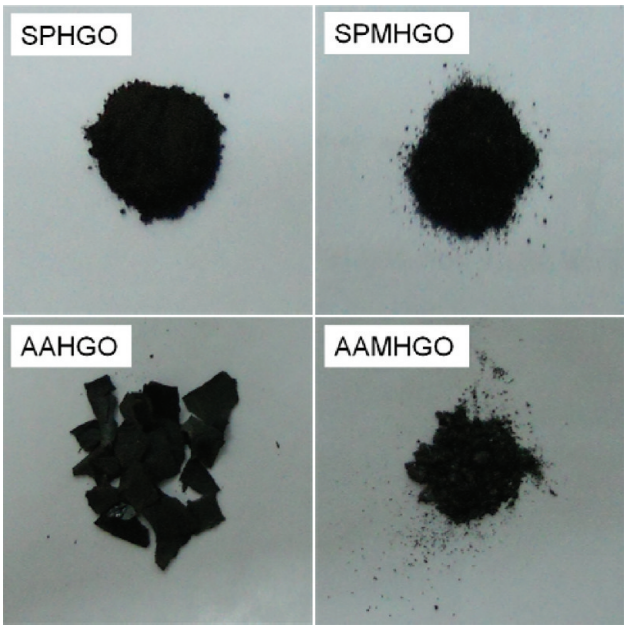

Figure 1. Graphite oxide (GO) prepared from SP graphite and AA graphite using Hummers method (H) and modified Hummers method (MH).

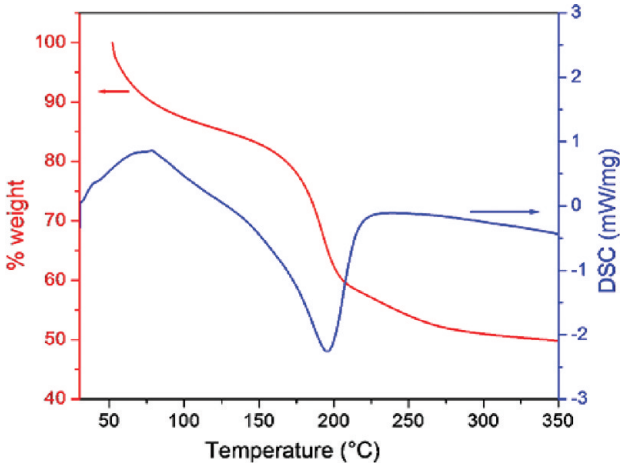

Figure 2. Thermogravimetric analysis (TGA, red curve) and differential scanning calorimetry (DSC, blue curve) of graphite oxide (GO) in nitrogen atmosphere.

The Hummers' method and its variant used in the present study for the synthesis of GO have been shown to completely destroy the layered structure of graphite, as is also observed in the present case. This happens due to the expansion caused by the introduction of oxygen-containing functional groups between the graphitic layers. To investigate the thermal behavior of GO at different temperatures, thermogravimetric analysis and differential scanning calorimetry (TG/DSC) of GO were carried out (Figure 2). Significant changes are observed in the TGA curve of GO below 350 °C. The presence of the functional groups and interlamellar water weakens the van der Waals interaction between the GO layers. Consequently, the TGA curve of GO (taken at 5 °C/min in N_2 atmosphere) shows two main regions with considerable weight loss, when scanned until 350 °C. The first small weight loss is below 100 °C and is due to the removal of adsorbed water from GO. The present GO contains ∼15% water, which was also confirmed by weighing the sample before and after drying. The removal of water is also confirmed from the DSC curve, which shows an endothermic peak below 100 °C corresponding to the evaporation of water. The main weight loss in GO occurs at ∼200 °C, which is due to the pyrolysis of the labile oxygen-containing functional groups.[30] The DSC signal also shows a marked exothermic peak at 200 °C, suggesting the removal of functional groups.

The functional groups that are generally believed to be present are hydroxyl, epoxide, carbonyl, alkyl, and carboxyl groups. The removal of these functional groups is the key idea behind the synthesis of graphene from GO. As shown in Figure 2, the maximum rate of evolution of oxygen from GO occurs at 200 °C. Yet, McAllister et al.[31] have suggested that for successful exfoliation the decomposition rate of the functional groups must exceed the diffusion rate of evolved gases. The pressure of the evolved gases at 200 °C may be sufficient to remove the oxygen from GO but is not enough to fully exfoliate the graphitic layers. The heating rate also plays a crucial role in exfoliation. Therefore, a preheated high temperature (1050 °C, 2000 °C/min, Ar atm) environment was proposed for successful exfoliation.[31] This method has come to be known as thermal exfoliation. However, Wei et al.[16] suggested that if the inner stress generated from the removal of oxygen-containing functional groups could be reinforced by providing a suitable atmosphere, then exfoliation can be achieved at a much lower temperature. They demonstrated a vacuum exfoliation technique wherein a high vacuum environment helps to accelerate exfoliation at lower temperature (∼200−400 °C). On similar lines, we proposed a novel hydrogen exfoliation technique in which the vigorous reaction between hydrogen- and oxygen-containing groups (mainly hydroxide) provides the extra energy needed to cause disruption of graphitic planes. We have also synthesized graphene by hydrogen−argon exfoliation at 200 °C, to study the effect of the different atmospheres on GO exfoliation-reduction. The idea behind GO exfoliation has been schematically presented in Figure 3.

3.2. Fourier Transform Infrared and UV−Visible Spectroscopy. To determine the functional groups present in the samples, FTIR spectroscopy studies were carried out. Figure 4a shows the FTIR spectrum of SPGr and SPHGO. Precursor graphite shows mostly adsorbed −OH peaks at ∼3442 cm^{-1}, CH_x doublet at 2922 and 2860 cm^{-1}, and C═C stretching at 1620 cm^{-1}.[32] A weak carbonyl group at 1720 cm^{-1} can also be seen for SPGr. GO consists of covalently attached oxygen-containing groups such as hydroxyl, epoxy, carbonyl, and carboxyl groups. The carboxyl group shows its presence throughout the spectra of GO in the form of a very broad −OH peak from 3600 to 2000 cm^{-1} (also includes the adsorbed water peak), strong C═O peak at 1720 cm^{-1}, strong C−O peak at 1230 cm^{-1}, and weak −OH bending at 1410 cm^{-1}.[33] The carbon backbone C═C stretch can be seen at 1620 cm^{-1} as in graphite. The broadening of the −OH peak is due to hydrogen bonding between the OH molecules. The C−O stretching vibration at 1050 cm^{-1} shows the presence of epoxy groups. It is generally accepted that the epoxy and −OH functional groups are attached above and below the basal planes, while the −COOH groups are bound to the edges of the basal planes. The FTIR peaks of exfoliated graphenes are presented in Figure 4b. Most of the functional groups are removed during the exfoliation-reduction represented by the decrease in the intensity of the peaks.

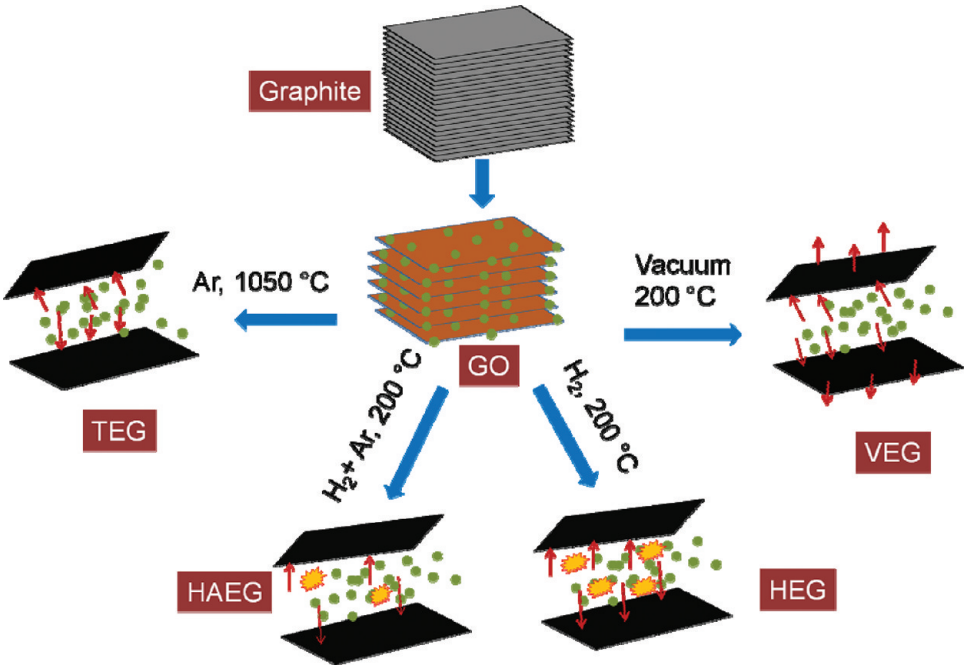

Figure 3. Schematic representation of the mechanisms involved in "gasothermal" exfoliation techniques.

The figure shows that O−H stretching vibrations observed at 3400 cm^{-1} are significantly reduced, especially in the case of HEG. In the case of C═O and C−O groups, the intensities are comparable for TEG, VEG, and HAEG, whereas it is significantly low for HEG. This supports the mechanism suggested in section 3.1 wherein during exfoliation in the presence of hydrogen, oxygen-containing functional groups are removed to a greater extent.

To further confirm the presence of these functional groups, UV−Visible spectroscopy was carried out on samples dispersed in ethanol (Figure 5). The UV−Vis spectrum of graphite oxide/graphene oxide exhibits two characteristic features that can be used as a means of identification: a maximum at ∼240 nm, corresponding to $\pi \rightarrow \pi^*$ transitions of C═C bonds;[34] and the shoulder peak at ∼300 nm can be attributed to $n \rightarrow \pi^*$ transitions of C═O bonds. $\pi \rightarrow \pi^*$ and $n \rightarrow \pi^*$ are bathochromically and hypochromically shifted by conjugation. Accordingly, on reduction to graphene by all four methods, the absorption peaks at 240 nm red-shifted to 270 nm. This red shift suggests that the electronic conjugation within the graphene sheets is restored upon exfoliation. The shoulder peak at 300 nm in GO is almost absent, suggesting the removal of C═O groups.

XPS analysis was also carried out to assess the presence of various functional groups in the samples. Figure 6a−e shows the deconvoluted C1s XPS spectra of Gr, GO, TEG, HAEG, and HEG. Because the sample preparation involved dispersing the samples in water, some undesirable hydroxyl group might have been introduced. Hence, this analysis is qualitative. Precursor graphite (Figure 6a) shows mainly a peak corresponding to sp^2 carbon network (C−C) at 284.7 eV along with a high energy tail, probably corresponding to −COOH and C═O group. The presence of these groups in graphite could be due to some pretreatment given to make it expandable graphite. In GO (Figure 6b), a significant amount of functional groups was introduced in the form of hydroxyl, carboxyl, and carbonyl. The peak at ∼286 eV comes from C−O. This could be the epoxide group (C−O−C) or the hydroxyl (C−OH), both of which have a similar C1s binding energy. The carboxyl and carbonyl groups are also present in GO to a considerable extent. In the case of exfoliated graphenes, significant reduction in the amount of functional groups was observed. In TEG (Figure 6d), due to high temperature treatment, most of the groups like −COOH, C═O, and C−OH are removed. The peak at 285.7 eV could be from the epoxide groups (C−O−C) as most of the adsorbed water is removed during exfoliation. It can also be seen that in TEG more C═O groups are removed than C−O−C. It is to be expected that when the temperature of exfoliation is lowered, less amount of functional groups will be removed. Accordingly, after exfoliation at 200 °C, HAEG (Figure 6c) shows a significant amount of functional groups as compared to TEG. However, it is interesting to note that when exfoliation is done in pure hydrogen atmosphere (HEG) even at a low temperature of 200 °C (Figure 6e), there is considerable reduction in the functional groups, especially the −OH and C−O−C groups.[35−37] This further supports the mechanism proposed in section 3.1. The peak positions corresponding to various functional groups are summarized in Table 1.

3.3. X-ray Diffractograms and Crystallite Size. The structural changes occurring during the conversion of graphite to graphene were studied using X-ray diffraction patterns. Figure 7 presents the XRD patterns of Gr, GO, and the different exfoliated graphenes (samples prepared from SPGr). Graphite has an intense crystalline peak at ∼26.5° corresponding to the (002) plane with a *d*-spacing of 0.335 nm. This sharp peak is due to the highly ordered stacking in graphite. On conversion to GO, the (002) graphitic peak shifts to ∼10.5°. This is due to the increase in the interlayer spacing due to the intercalation of oxygen-containing functional groups and water between the graphitic layers, because $d \propto 1/\sin(\theta)$. For SPHGO, the *d*-spacing is ∼0.84 nm. Reported values vary between 0.7 and 0.9 nm depending on the amount of intercalation.[38,39] After exfoliation, the GO diffraction peak disappears and is replaced by a broad peak in the 2θ range of 14−30° for all graphenes.[18] In graphene,

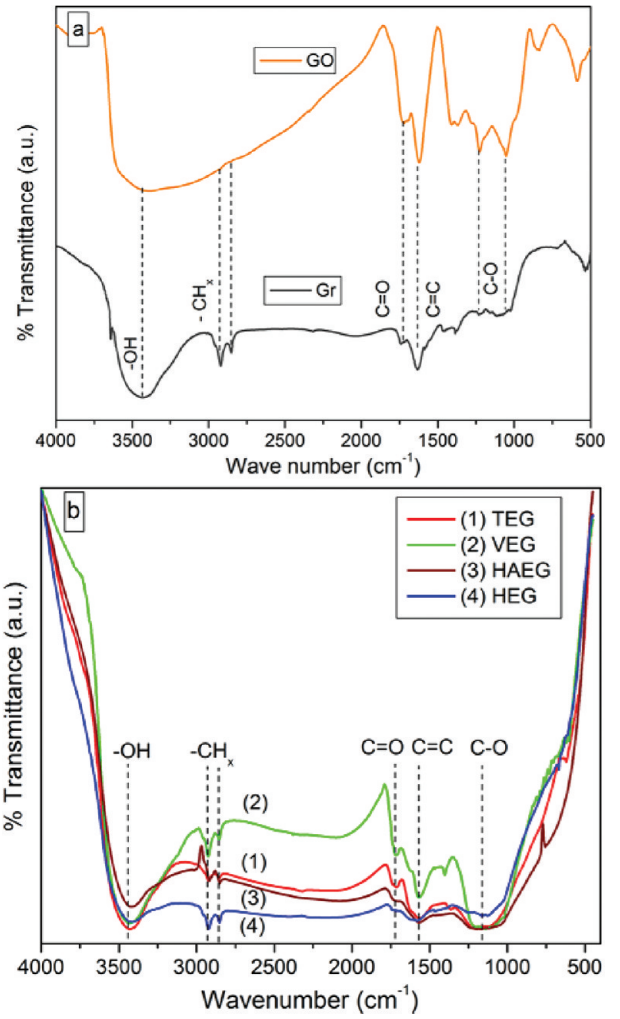

Figure 4. Fourier transform infrared spectra of (a) graphite (Gr) and graphite oxide (GO), and (b) thermally exfoliated graphene (TEG), vacuum exfoliated graphene (VEG), hydrogen−argon exfoliated graphene (HAEG), and hydrogen exfoliated graphene (HEG).

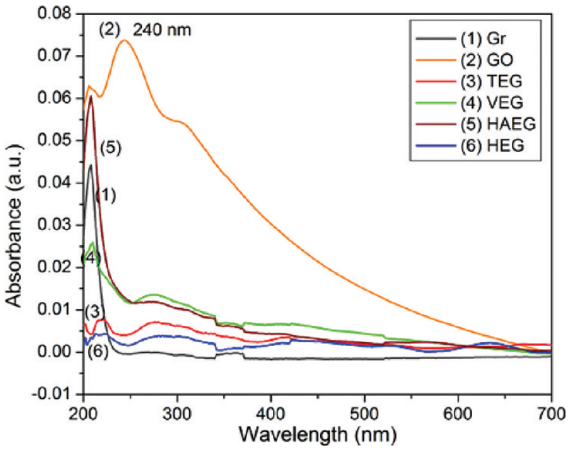

Figure 5. UV−vis spectra of (a) graphite (Gr) and graphite oxide (GO), and (b) thermally exfoliated graphene (TEG), vacuum exfoliated graphene (VEG), hydrogen−argon exfoliated graphene (HAEG), and hydrogen exfoliated graphene (HEG).

interlayer spacing decreases to ∼0.36−0.37 nm, close to the value of pristine graphite, indicating the removal of oxygen and water during exfoliation. This broad peak is also suggestive of the loss of the long-range order in graphenes. These diffraction patterns were taken on glass substrates, which also have an amorphous-like peak, similar to the graphenes. However, we have checked the broadening and peak position of graphenes by taking the diffraction patterns on aluminum substrates but found little deviation from the values reported.

We propose that a rough estimate of the maximum number of layers in graphene sheets can be obtained from the broadening of the diffraction peaks. The details for obtaining the same are given in the Supporting Information. From the data given in Table S1, it can be seen that SP graphite (SPGr) has more than 100 layers, whereas the ball milled AA graphite (AAGr) has around 250 layers, separated by *d*-spacing of 0.335 nm. All of the GOs prepared have 10−15 layers separated by ∼0.8 nm. Surprisingly, all of the graphenes, that is, TEG, VEG, HAEG, and HEG, have ∼5 layers each, in the powder form. One must bear in mind that this estimates only the upper bound on the number of layers. Generally, a distribution in the number of layers would exist, and the maxima of this distribution will depend on the exfoliation technique. It is interesting to note the (002) peak position shift in graphenes (indicated by the dotted line in Figure 7). As far as we know, there is no observation of such kind in the literature. The peak position shifts from 24.8° in TEG to 24.2° in VEG and 23.9° in HAEG, whereas in HEG it is ∼25.2°. We believe this shift in the peaks is an indicator of the amount of oxygen present. As the oxygen content increases, the peak shifts toward that of GO. Because most of the oxygen is removed during exfoliation, the peak shift is not very high. In the case of HEG, the peak shifts away from that of GO and closer to that of graphite, indicating a higher oxygen removal. Thus, the oxygen content of the graphenes is in the following order: HAEG > VEG > TEG > HEG. Further support for the above hypothesis can be obtained from later sections on conductivity and elemental analysis.

3.4. Raman Spectroscopy of Exfoliated Graphene. The Raman spectrum of sp^2 carbons like graphene has been under intense investigation as it can provide valuable information regarding the crystallite size, the presence of sp^2-sp^3 hybridization, doping, defects, crystal disorder, edge structure, number of graphene layers, etc.[40] Upon careful investigation of the extensive literature available, it appears that the Raman spectra are particularly sensitive to the presence of sp^3 defects and disorder. The Raman spectra of different exfoliated graphenes (EGs) are shown in Figure 8. The highly defective EGs (due to the harsh oxidation and exfoliation processes) show a prominent D (disorder) band at ∼1350 cm^{-1}. The G band that corresponds to the sp^2 carbons occurs at ∼1580 cm^{-1} but is highly broadened, probably due to the presence of defects or reduction in crystallite size.[41] The G′ band, also known as the 2D band, is a Raman allowed mode for sp^2 carbons and occurs at ∼2700 cm^{-1}. It arises due to a double resonance phonon scattering process and is strongly affected by any perturbation to the electronic/phonon structure of graphene. In the case of EGs, the intensity of the 2D band is significantly low. This can be attributed to the presence of disorder, which makes the EGs highly wrinkled, in effect reducing the effective planar component of graphene. This very low intensity of the 2D band in case of EGs is well supported by literature.[42−44] Further discussions on the Raman spectra of Gr, GO, and HEG are given in our previous work.[18]

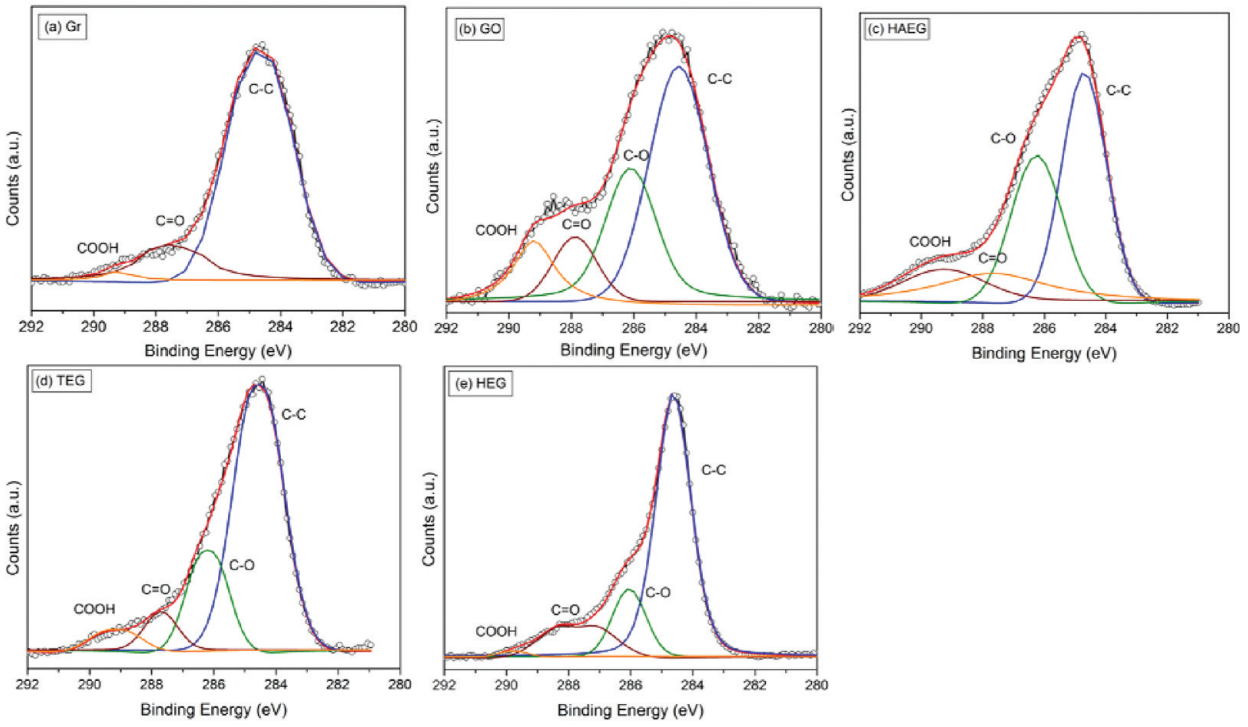

Figure 6. C1s XPS spectra of (a) graphite (Gr), (b) graphite oxide (GO), (c) hydrogen−argon exfoliated graphene (HAEG), (d) thermally exfoliated graphene (TEG), and (e) hydrogen exfoliated graphene (HEG). The peaks were deconvoluted into peaks of C−C, C−OH, C−O−C, C═O, and COOH groups.

Table 1. Peak Positions of Various Groups in C1s Spectra of Graphite (Gr), Graphite Oxide (GO), and "Gasothermally" Exfoliated Graphene[a]

	functional group peak positions (eV)			
sample	C═C	C−O	C═O	COOH
Gr	284.6		287.5	289.2
GO	284.6	286.1	287.9	289.2
HAEG	284.7	286.2	287.7	289.3
TEG	284.6	286.2	287.7	289.2
HEG	284.6	286.1	287.8	289.2

[a] TEG, thermally exfoliated graphene; HAEG, hydrogen−argon exfoliated graphene; HEG, hydrogen exfoliated graphene.

3.5. Electron Microscopy. The surface morphology of graphite, graphite oxide, and graphene was studied using field emission scanning electron microscopy. Figure 9a−f shows the FESEM images of Gr, GO, TEG, VEG, HAEG, and HEG. In all images, the scale is 1 μm. As expected, graphite shows a layered and three-dimentional nature. The thick edges of graphite indicate that there are about 100 graphene sheets in a graphite flake. Unlike graphite, GO shows a disordered morphology, which indicates that after the oxidation of graphite, its crystal structure is disturbed. The exfoliation of GO is clear from the images and can be seen in the form of separation induced between the graphene sheets. As a result of this exfoliation, the "gasothermal" graphenes show a wrinkled and fluffy morphology. The high resolution transmission electron microscopy image and select area electron diffraction (SAED) pattern of HEG are shown in Figure 9g,h. The image shows the individual graphene sheets as well as the folding at the edges. The wrinkled morphology is clearer in the TEM image. Similar morphologies were observed for the other "gasothermal" graphenes also. The SAED image shows weak and diffuse rings, indicating the loss of long-range ordering in graphene sheets.[45]

3.6. Surface Area Determination. The surface area of the as-grown powdered graphene was determined by BET surface area measurements. The N_2 adsorption desorption isotherms for TEG and HEG are presented in Figure 10. The isotherms exhibits type-II pattern and type H3 hysteresis loop. The presence of adsorption hysteresis suggests that the isotherm is a pseudo type-II pattern.[46] Generally, this kind of behavior is observed due to multilayer adsorption in materials having slit-like pores or aggregates of platy particles. Graphene sheets due to their few layered nature have slit-like open pores. Adsorption occurs on the surface of the graphene sheets and also in these pores. These open pores are responsible for hysteresis loop observed in graphene materials.[47] From the linear region of the graphs and using the BET equation, the BET specific surface area was determined to be 470 and 443 m^2/g for TEG and HEG, respectively. The surface area of VEG, on the other hand, has been reported as 350 m^2/g.[16]

The BET method of surface area measurement depends on the interaction of nitrogen gas with the powdered material. In exfoliated graphenes, the full surface might not be available for adsorption of gas and hence may not show their true surface area. To get a better estimation of the surface area, the methylene blue (MB) adsorption method was used. The use of MB dye as an indicator of surface areas of graphitic materials has been reported in previous studies.[15,48] In the present case, this analysis was carried out only for HEG. Known amounts of HEG were dispersed in aqueous MB by ultrasonication and left to settle.

dx.doi.org/10.1021/jp204039k |J. Phys. Chem. C 2011, 115, 17660–17669

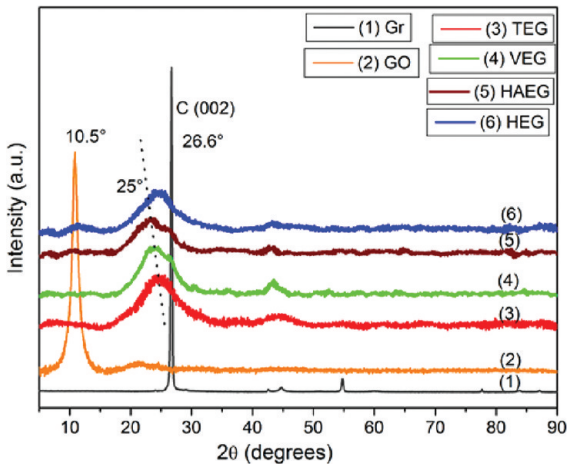

Figure 7. XRD patterns of graphite (Gr), graphite oxide (GO), thermally exfoliated graphene (TEG), vacuum exfoliated graphene (VEG), hydrogen−argon exfoliated graphene (HAEG), and hydrogen exfoliated graphene (HEG).

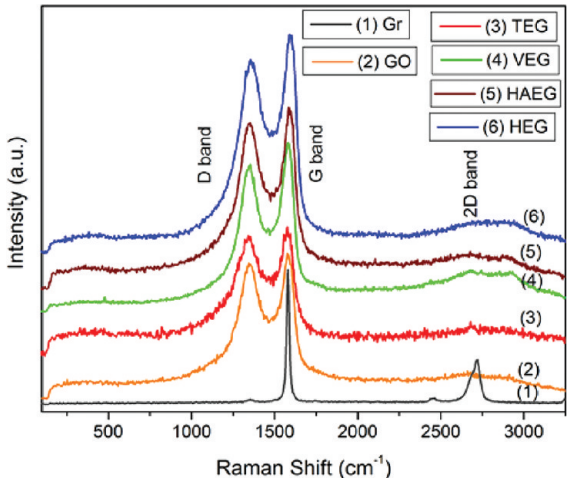

Figure 8. Raman spectra of graphite (Gr), graphite oxide (GO), thermally exfoliated graphene (TEG), vacuum exfoliated graphene (VEG), hydrogen−argon exfoliated graphene (HAEG), and hydrogen exfoliated graphene (HEG).

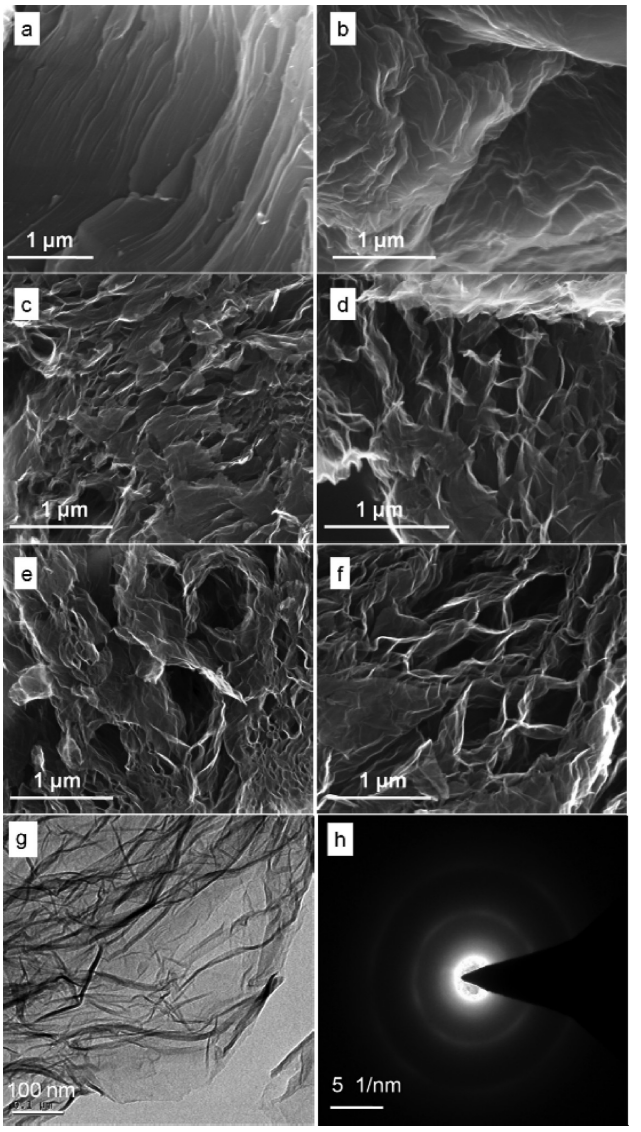

Figure 9. Field emission scanning electron microscopy images of (a) graphite (Gr), (b) graphite oxide (GO), (c) thermally exfoliated graphene (TEG), (d) vacuum exfoliated graphene (VEG), (e) hydrogen−argon exfoliated graphene (HAEG), and (f) hydrogen exfoliated graphene (HEG). (g) High resolution transmission electron microscopy image of HEG showing its wrinkled morphology and (h) select area electron diffraction pattern of HEG showing the loss of long-range ordering.

During ultrasonication, some of the loosely bound sheets further separate, providing greater surface area for adsorption. The adsorption of the dye occurs on the entire exposed surface of graphene, resulting in a decrease in the concentration of the original dye solution. The concentration of MB in each solution was then determined by UV−Vis spectroscopy. Using standard analysis methods, a Langmuir adsorption plot was then obtained. Using the y-intercept $(1/X_m)$ value obtained from the Langmuir plot, the surface area (S) was calculated using the equation, $S = X_m \times N \times a$, where N is Avogadro's number and a is the area of the absorbing molecule. Thus, the surface area of HEG was estimated to be ∼1697 m^2/g. This value is close to the value of surface area of single layer graphene, which is ∼2600 m^2/g.

3.7. Elemental Analysis and Electrical Conductivity Measurements. Energy dispersive X-ray analysis (EDX) was carried out for the estimation of the elemental composition in all of the samples. EDX was taken at a minimum of six different locations on the samples, and the values were averaged to estimate the carbon and oxygen content in each sample. The weight percentage and atomic percentage of carbon and oxygen and C/O ratio for Gr, GO, HAEG, VEG, TEG, and HEG are given in Table S2 in the Supporting Information. Gr has the highest C/O ratio of ∼37, which decreases drastically in GO to a value of ∼2.3. The exfoliated graphenes have C/O ratios in the flowing order: HEG > TEG > VEG > HAEG. HEG has the highest C/O ratio of ∼14.6, suggesting that exfoliation in pure hydrogen atmosphere removes a significant amount of oxygen-containing functional groups. This is in conformity with the XRD, FT-IR, UV−Visible, and XPS analyses in the previous sections. A rough estimate of the percentage of carbon content in the samples was obtained from XPS analyses also. This was obtained from the area

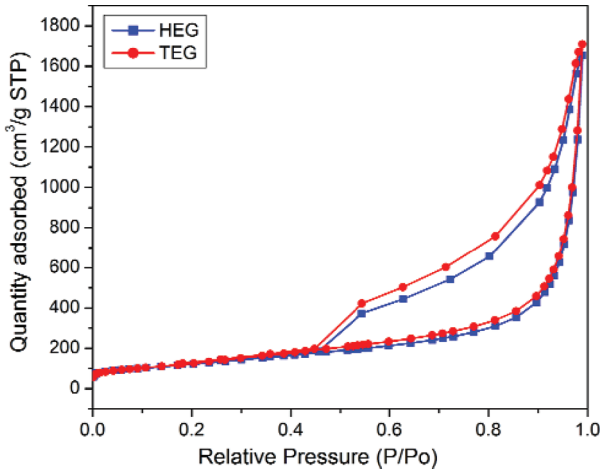

Figure 10. Nitrogen adsorption desorption isotherms for thermally exfoliated graphene (TEG, red ●) and hydrogen exfoliated graphene (HEG, blue ■).

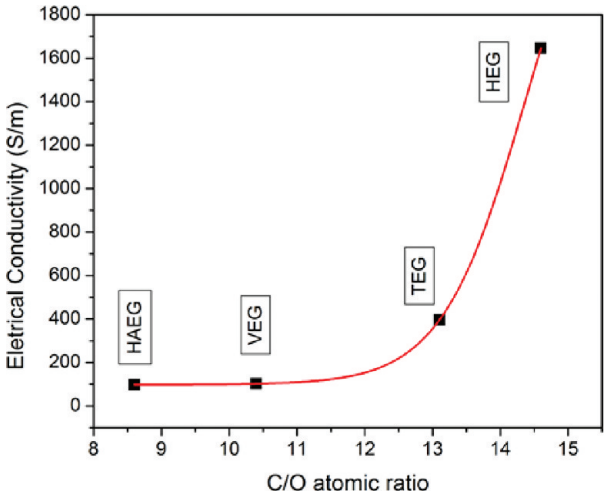

Figure 11. Variation of electrical conductivity of "gasothermally" exfoliated graphenes. The connecting red line is a guide to the eye.

Table 2. Electrical Conductivity of the Graphite (Gr), Graphite Oxide (GO), and "Gasothermally" Exfoliated Graphenes[a]

no.	sample	conductivity (S/m)
1	Gr	2.48×10^4
2	GO	6.65×10^{-4}
3	TEG	3.95×10^2
4	VEG	1.02×10^2
5	HAEG	9.76×10^1
6	HEG	1.64×10^3

[a] TEG, thermally exfoliated graphene; HAEG, hydrogen−argon exfoliated graphene; HEG, hydrogen exfoliated graphene.

percentages of various peaks and their relative contribution to carbon in the respective C1s spectra of the materials. The carbon content varies as follows: GO (63.3%), HAEG (78.1%), TEG (88.4%), and HEG (89.2%), which is in close agreement with the values obtained from EDX.

Electrical conductivity of the samples was measured via the linear four-probe method. The results are presented in Table 2. Pristine graphite has a high electrical conductivity of $\sim 10^4$ S/m. The reported values for graphite vary between 10^4 and 10^5 S/m.[49] This large value of conductivity is due to its high crystallinity and delocalized electrons. This is the average electrical conductivity of the powder and not the conductivity along the $a-b$ plane or along the c-axis. When oxidized to GO, the conductivity decreases by a large extent to $\sim 10^{-4}$ S/m. This is due to the presence of adsorbed water and a large amount of oxygen-containing functional groups between the graphitic planes. As mentioned earlier, in gasothermal exfoliation techniques, reduction and exfoliation happen simultaneously. Accordingly, the conductivity of graphene sample is 10^6-10^7 times higher than that of GO. The electrical conductivities of different graphenes are in the following order: HEG > TEG > VEG > HAEG. The differences in the electrical conductivity may be related to the differences in the oxygen content of the samples. Figure 11 shows the variation of the electrical conductivity with C/O atomic ratio for graphene samples. A sharp increase in the conductivity can be seen as the oxygen content decreases. The role of specific functional groups in determining the electrical conductivity is not yet clear. Nevertheless, as can be seen from the area percentages of various groups in XPS spectra, HEG has the least amount of −OH and C−O−C groups. TEG has the lowest C═O content, but it has higher C−O−C content as compared to HEG. This could possibly be the reason for its lower electrical conductivity as compared to HEG. Further studies are required to understand the effect of C−O−C and C═O bonds on the electrical conductivity of graphene samples. Thus, the conductivity measurements prove beyond doubt that exfoliation-reduction in hydrogen atmosphere is superior to other gasothermally exfoliated graphenes. This also supports our hypothesis that the shift in the (002) XRD peak of exfoliated graphenes is a qualitative measure of the oxygen content in the samples and therefore suggestive of their electrical conductivities.

3.8. Criticality of Exfoliation. Successful exfoliation-reduction of GO is a very critical process, especially at lower temperatures. The atmosphere during exfoliation plays a crucial role in determining the final quality of graphene. Gaseous atmospheres generally assist in volume expansion, and a reducing atmosphere will be helpful in the removal of functional groups. In solution-based methods, the liquid media prevent volume expansion. Nonetheless, if these processes are well controlled, high-quality planar and wrinkle free graphene can be obtained. For comparison, we have synthesized graphene by hydrazine reduction, and the results have been discussed in the Supporting Information. Another critical requirement for exfoliation is that the process must be "instantaneous" and "simultaneous". This is to mean that at the critical point of exfoliation, all GO particles should exfoliate at the same time because there is a possibility that some GO particles may simply get reduced to graphite-like structures. In such cases, the sample will have mixed phases of graphene, GO, and graphite. This is particularly true for methods that involve exfoliation of GO powder using focused energy such as flash, microwave, etc. Only GO that is exposed gets exfoliated. We performed microwave exfoliation of GO powders, and the results that have been presented in the Supporting Information support the hypothesis. The problem of non uniform exfoliation can be overcome by carrying out exfoliation of GO in suitable solvents. In the "gasothermal" methods, critical issues are maintaining a

uniform temperature and safe handling of gases. Provided these issues are addressed, simple modifications can be done to the above techniques to facilitate large-scale graphene synthesis. We present two simple modifications: hydrogen exfoliation on a hot plate and vacuum exfoliation in a vacuum oven. These have been discussed in the Supporting Information.

4. CONCLUSION

Low temperature exfoliation-reduction of graphene is a critical process wherein the atmosphere maintained during exfoliation plays a crucial role in determining the quality of the graphene sheets. Among the different gaseous atmospheres used, exfoliation in pure hydrogen atmosphere results in a considerable decrease in the amount of oxygen-containing functional groups. Consequently, the electrical conductivity of HEG is the highest among the exfoliated graphenes. A rule of thumb method for determining the upper bound on the number of layers in few layered graphene based on X-ray diffraction has also been suggested. Our results conclusively show that high-quality graphene sheets can be obtained by hydrogen exfoliation at a low temperature, thereby facilitating large-scale industrial applications of graphene.

■ ASSOCIATED CONTENT

Supporting Information. Details of XRD analysis, discussion on the properties of chemically and microwave exfoliated graphene, elaboration of facile methods for "gasothermal" graphene production, and electrochemical study of graphenes. This material is available free of charge via the Internet at http://pubs.acs.org.

■ AUTHOR INFORMATION

Corresponding Author
*E-mail: ramp@iitm.ac.in.

■ ACKNOWLEDGMENT

We thank the Indian Institute of Technology Madras (IITM), India, and Department of Science and Technology, India, for supporting the research in terms of finance, facilities, and infrastructure.

■ REFERENCES

(1) Zhang, Y. B.; Tan, Y. W.; Stormer, H. L.; Kim, P. *Nature* **2005**, *438*, 201–204.
(2) Kane, C. L.; Mele, E. J. *Phys. Rev. Lett.* **2005**, *95*, 226801.
(3) Morozov, S. V.; Novoselov, K. S.; Katsnelson, M. I.; Schedin, F.; Ponomarenko, L. A.; Jiang, D.; Geim, A. K. *Phys. Rev. Lett.* **2006**, *97*, 016801.
(4) Pisana, S.; Lazzeri, M.; Casiraghi, C.; Novoselov, K. S.; Geim, A. K.; Ferrari, A. C.; Mauri, F. *Nat. Mater.* **2007**, *6*, 198–201.
(5) Novoselov, K. S.; Geim, A. K.; Morozov, S. V.; Jiang, D.; Zhang, Y.; Dubonos, S. V.; Grigorieva, I. V.; Firsov, A. A. *Science* **2004**, *306*, 666–669.
(6) Novoselov, K. S.; Geim, A. K.; Morozov, S. V.; Jiang, D.; Katsnelson, M. I.; Grigorieva, I. V.; Dubonos, S. V.; Firsov, A. A. *Nature* **2005**, *438*, 197–200.
(7) Peres, N. M. R.; Castro Neto, A. H.; Guinea, F. *Phys. Rev. B* **2006**, *73*, 195411.
(8) Geim, A. K.; Novoselov, K. S. *Nat. Mater.* **2007**, *6*, 183–191.
(9) Hass, J.; Feng, R.; Li, T.; Li, X.; Zong, Z.; de Heer, W. A.; First, P. N.; Conrad, E. H.; Jeffrey, C. A.; Berger, C. *Appl. Phys. Lett.* **2006**, *89*, 143106.
(10) Green, A. A.; Hersam, M. C. *Nano Lett.* **2009**, *9*, 4031–4036.
(11) Eda, G.; Unalan, H. E.; Rupesinghe, N.; Amaratunga, G. A. J.; Chhowalla, M. *Appl. Phys. Lett.* **2008**, *93*, 233502.
(12) Hernandez, Y.; Nicolosi, V.; Lotya, M.; Blighe, F. M.; Sun, Z.; De, S.; Mcgovern, I. T.; Holland, B.; Byrne, M.; Gun'ko, Y. K.; et al. *Nat. Nanotechnol.* **2008**, *3*, 563–568.
(13) Viculis, L. M.; Mack, J. J.; Mayer, O. M.; Hahn, H. T.; Kaner, R. B. *J. Mater. Chem.* **2005**, *15*, 974–978.
(14) Zhu, Y.; Murali, S.; Stoller, M. D.; Velamakanni, A.; Piner, R. D.; Ruoff, R. S. *Carbon* **2010**, *48*, 2118–2122.
(15) Schniepp, H. C.; Li, J. L.; McAllister, M. J.; Sai, H.; Alonso, M. H.; Adamson, D. H.; Prud'homme, R. K.; Car, R.; Saville, D. A.; Aksay, I. A. *J. Phys. Chem. B* **2006**, *110*, 8535–8539.
(16) Lv, W.; Tang, D.-M.; He, Y.-B. *ACS Nano* **2009**, *3*, 3730–6.
(17) Wu, Z.-S.; Ren, W.; Gao, L.; Liu, B.; Jiang, C.; Cheng, H.-M. *Carbon* **2009**, *47*, 493–499.
(18) Kaniyoor, A.; Baby, T. T.; Ramaprabhu, S. *J. Mater. Chem.* **2010**, *20*, 8467–8469.
(19) Gao, W.; Alemany, L. B.; Ci, L.; Ajayan, P. M. *Nat. Chem.* **2009**, *1*, 403–408.
(20) Murugan, A. V.; Muraliganth, T.; Manthiram, A. *Chem. Mater.* **2009**, *21*, 5004–5006.
(21) Lin, Z.; Yao, Y.; Li, Z.; Liu, Y.; Li, Z.; Wong, C.-P. *J. Phys. Chem. C* **2010**, *114*, 14819–14825.
(22) Choucair, M.; Thordarson, P.; Stride, J. A. *Nat. Nanotechnol.* **2009**, *4*, 30–33.
(23) Abdelsayed, V.; Moussa, S.; Hassan, H. M.; Aluri, H. S.; Collinson, M. M.; El-Shall, M. S. *J. Phys. Chem. Lett.* **2010**, *1*, 2804–2809.
(24) Subrahmanyam, K. S.; Kumar, P.; Nag, A.; Rao, C. N. R. *Solid State Commun.* **2010**, *150*, 1774–1777.
(25) Somani, P. R.; Somani, S. P.; Umeno, M. *Chem. Phys. Lett.* **2006**, *430*, 56–59.
(26) Gullapalli, H.; Reddy, A. L. M.; Kilpatrick, S.; Dubey, M.; Ajayan, P. M. *Small* **2011**, *7*, 1697–1700.
(27) Reddy, A. L. M.; Srivastava, A.; Gowda, S. R.; Gullapalli, H.; Dubey, M.; Ajayan, P. M. *ACS Nano* **2010**, *4*, 6337–6342.
(28) Malesevic, A.; Vitchev, R.; Schouteden, K.; Volodin, A.; Zhang, L.; Tendeloo, G. V.; Vanhulsel, A.; Haesendonck, C. V. *Nanotechnology* **2008**, *19*, 305604.
(29) Ramaprabhu, S.; Rajalakshmi, N.; Weiss, A. *Int. J. Hydrogen Energy* **1998**, *23*, 797–801.
(30) Ren, P.-G.; Yan, D.-X.; Ji, X.; Chen, T.; Li, Z.-M. *Nanotechnology* **2011**, *22*, 055705.
(31) McAllister, M. J.; Li, J.-L.; Adamson, D. H.; Schniepp, H. C.; Abdala, A. A.; Liu, J.; Alonso, M. H.; Milius, D. L.; Car, R.; Prud'homme, R. K.; et al. *Chem. Mater.* **2007**, *19*, 4396–4404.
(32) Jeong, H.-K.; Colakerol, L.; Jin, M. H.; Glans, P.-A.; Smith, K. E.; Lee, Y. H. *Chem. Phys. Lett.* **2008**, *460*, 499–502.
(33) Jeong, H.-K.; Lee, Y. P.; Jin, M. H.; Kim, E. S.; Bae, J. J.; Lee, Y. H. *Chem. Phys. Lett.* **2009**, *470*, 255–258.
(34) Li, D.; Müller, M. B.; Gilje, S.; Kaner, R. B.; Wallace, G. G. *Nat. Nanotechnol.* **2008**, *3*, 101–105.
(35) Lotya, M.; Hernandez, Y.; King, P. J.; Smith, R. J.; Nicolosi, V.; Karlsson, L. S.; Blighe, F. M.; De, S.; Wang, Z.; McGovern, I. T.; Duesberg, G. S.; Coleman, J. N. *J. Am. Chem. Soc.* **2009**, *131*, 3611–3620.
(36) Jin, M.; Jeong, H.-K.; Kim, T.-H.; So, K. P.; Cui, Y.; Yu, W. J.; Ra, E. J.; Lee, Y. H. *J. Phys. D: Appl. Phys.* **2010**, *43*, 275402–275408.
(37) Wang, Y.; Shao, Y.; Matson, D. W.; Li, J.; Lin, Y. *ACS Nano* **2010**, *4*, 1790–1798.
(38) Xiong, Z.; Zhang, L. L.; Ma, J.; Zhao, X. S. *Chem. Commun.* **2010**, *46*, 6099–6101.
(39) Gao, Y.; Ma, D.; Wang, C.; Guan, J.; Bao, X. *Chem. Commun.* **2011**, *47*, 2432–2449.
(40) Tuinstra, F.; Koenig, J. L. *J. Chem. Phys.* **1970**, *53*, 1126–1130.
(41) Zickler, G. A.; Smarsly, B.; Gierlinger, N.; Peterlik, H.; Paris, O. *Carbon* **2006**, *44*, 3239–3246.
(42) Ai, K.; Liu, Y.; Lu, L.; Cheng, X.; Huo, L. *J. Mater. Chem.* **2011**, *21*, 3365–3370.

(43) Kudin, K. N.; Ozbas, B.; Schniepp, H. C.; Prud'homme, R. K.; Aksay, I. A.; Car, R. *Nano Lett.* **2008**, *8*, 36–41.
(44) Liu, J.; Jeong, H.; Liu, J.; Lee, K.; Park, J.-Y.; Ahn, Y. H.; Lee, S. *Carbon* **2010**, *48*, 2282–2289.
(45) Wang, G.; Yang, J.; Park, J.; Gou, X.; Wang, B.; Liu, H.; Yao, J. *J. Phys. Chem. C* **2008**, *112*, 8192–8195.
(46) Freeman, J. J.; Gimblett, E. G. R.; Roberts, R. A.; Sing, K. S. W. *Carbon* **1987**, *25*, 559–563.
(47) Sing, K. S. W. *J. Porous Mater.* **1995**, *2*, 5–8.
(48) Boehm, H. P.; Clauss, A.; Fisher, G. O.; Hofmann, U. *ZAAC* **1962**, *316*, 119–127.
(49) Buerschaper, R. A. *J. Appl. Phys.* **1944**, *15*, 452.